

Original Study

Open Access

Andrzej Helowicz*

Impact of subgrade and backfill stiffness on values and distribution of bending moments in integral box bridge

<https://doi.org/10.2478/sgem-2021-0001>

received March 26, 2020; accepted January 31, 2021.

Abstract: The article presents parametric analysis regarding the impact of subgrade and backfill stiffness on values and distribution of bending moments in the structural elements of a small integral box bridge made of cast in situ reinforced concrete. The analyzed parameters are the modulus of subgrade reaction under and behind the bridge structure (k_v , k_h). At the beginning, the author presents the integral box bridge and selected parts of the bridge design. In particular, the author focuses on the method of modeling of the subgrade stiffness parameters under and behind the bridge structure, as well as their impact on the values and distribution of bending moments in the bridge structural elements. The bridge was designed by the author and built on the M9 motorway between the towns of Waterford and Kilcullen in Ireland. In conclusions, the author shares his knowledge and experience relating to the design of small integral bridges and culverts and puts forward recommendations as to further research on these type of structures in Poland.

Keywords: precast box bridge; integral bridge; design; single-span bridge.

1 Introduction

An integral bridge can be defined as a bridge whose span is monolithically connected with the abutment walls and whose structure interacts with the surrounding soil due to thermal effects as well as various dead and live loads. Such elements as bridge bearings, mechanical expansion joints, and approach slabs are not required in this case, whereby the construction and maintenance of integral

bridge are less expensive. Integral bridge structures have been widely used in the world since the 1930s. This paper presents parametric analysis regarding the impact of subgrade and backfill stiffness on values and distribution of bending moments in the integral box bridge structure elements made of cast in situ reinforced concrete. In the analysis is used one of the diagrams of load cases proposed in standard [8]. The design and construction of this bridge is described more thoroughly in publication [5]. Other types of integral bridges and viaducts, both single-span and multi-span ones, and arch bridges are described in [1–4]. It is worth noting that the implementation of integral bridges on this section of the motorway contributed to a significant reduction in the time and cost of construction of the motorway.

2 Description of bridge structure

The integral box bridge structure located in County Kilkenny in Ireland on the M9 motorway connecting the towns of Kilcullen and Waterford (Figs. 1–3) is described. The main purpose of this bridge is to pass agricultural traffic, agricultural machinery, and livestock to the pastures separated by the motorway. The bridge was designed in accordance with the guidelines for bridges and road culverts. The traffic loads and the load configuration conformed to the Irish standard for bridges and culverts. The bridge was designed as integral with the surrounding soil. The parameters of the subgrade and the backfill used to build the bridge were specified by a geotechnical engineer. These parameters are presented in the impact analysis below. The grading requirement for the 6N/6P class materials used to backfill the structure is given in Table 2 [14]. The bridge carries a motorway with two one-way carriageways, each 7 m wide, separated by a 2.6 m wide median strip with a concrete Jersey barrier. At the outer edge of each of the two carriageways, there is a 2.5 m wide shoulder limited by a steel safety barrier. A 4.0

*Corresponding author: Andrzej Helowicz, Faculty of Civil Engineering, Wrocław University of Technology, E-mail: andrzej.helowicz@pwr.edu.pl

Table 1: Basic bridge parameters.

Elements	
Effective span length	$L_t=6.45$ [m]
Overall span length	$L_p=6.9$ [m]
Skew angle	$a=90^\circ$
Wall, upper floor slab, and bottom slab thickness	$h=0.45$ [m]
Minimal soil surcharge height over bridge structure	$H_n=1.1$ [m]
Length of bridge without wing walls	$L_o=30.6$ [m]
Overall length of wing walls	$L_s=8.49$ [m]
Angle of rotation of wing walls relative to bridge length	$b=45^\circ$
Span height to length ratio	1:15
Embankment height	6.0 [m]
Bottom slab and wing wall strip footing concrete class	C32/40
Bridge wall, upper floor slab, wing wall, and string course concrete class	C40/50
Live load type	HA and HB45



Figure 3: Bridge location (Microsoft Bing Maps) [18]

m wide road with two 1.0 m wide sidewalks adjacent to it runs under the bridge. The embankment over the bridge wing walls are protected with timber post and rail fencing with wire mesh. The basic parameters of the bridge are specified in Table 1.

The design documentation was prepared in the Fehily Timoney and Company consulting office in Cork [13]. Working for Fehily Timoney and Company, the author designed this bridge.

The following standards, among others, were used to design the bridge:

- BD31/01 The Design of Buried Concrete Box and Portal Frame Structures [8],
- BA42/96 The Design of Integral Bridges [9],
- BD37/01 Loads for Highway Bridges [10],
- BS5400-04 Code of practice for design of concrete bridges [11].

In addition, the Irish Manual of Contract Documents for Road Works [14] and the project owner’s (National Road Authority [12]) latest recommendations were used for the bridge design. Considering the interaction between the bridge and the surrounding soil, components, such as the backfill behind the bridge walls and the subgrade stiffness calculation, are described in the following section.

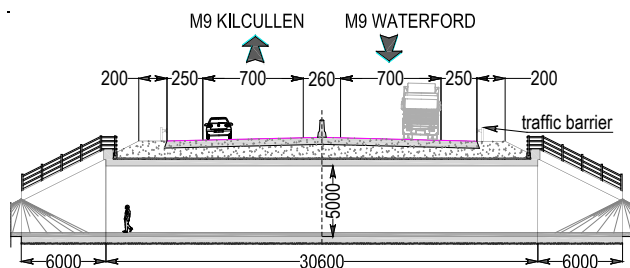


Figure 1: Longitudinal section of the bridge.

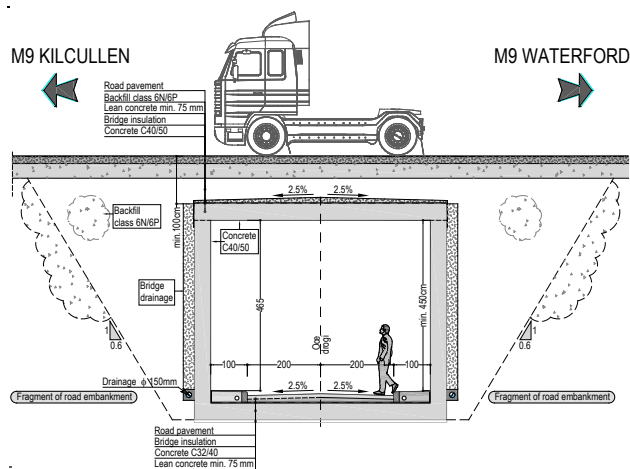


Figure 2: Cross-section of the bridge.

3 Backfill behind bridge abutment walls

The class of material used to bury integral bridges and the way of built-in it has have a significant impact on the distribution of internal forces in the bridge structure elements. For this purpose, class 6N and 6P backfill materials are used on the British Isles. These materials usually consist of crushed rock, crushed concrete, natural gravel, crushed gravel, or combination of both, excluding

Table 2. Grading of 6N and 6P class backfills [14].

Square mesh sieve [mm]	Percent passing sieve [%]	
	6N	6P
125		100
100	100	
75	65–100	
37,5	45–100	
10	15–75	
5	10–60	
0.6	0–30	
0.063	0–15	

argillaceous gravel aggregate. Detailed information about the backfills is given in the Manual of Contract Documents for Road Works [14] (Table 2). During the construction of the considered bridge, the effective angle of shearing resistance of the backfill ranged from $f=35^{\circ}$ to 40° .

It is important that before a bridge structure design begins, geotechnical investigations are carried out in the location where the future supports will be located, the modulus of subgrade reaction is determined, and the settlement of the supports is calculated. On the basis of this information, the designer can create a numerical model of the bridge structure, which will most accurately describe the actual foundation conditions. The model represents a structure on elastic supports, which behave flexibly, influenced by applied permanent and live loads. Moreover, if the stiffness of the structural members is low, the structure is flexible and better interacts with the surrounding soil, whereby the stresses in the structure elements are reduced and evenly distributed. For this reason, the cross-sections of the structural members of integral bridges can be smaller, whereby such bridges are less expensive to build than other types of bridges.

4 Permanent loads

Only permanent loads were used in the parametric analysis. Considering the permanent character of the load, the shape of the bridge was assumed to be invariable along its length, and to simplify the calculations a two-dimensional structure with beam elements was adopted as the model of the bridge structure. The loads were applied to the bridge model according to one of the load cases diagrams given in standard [8]. The standard

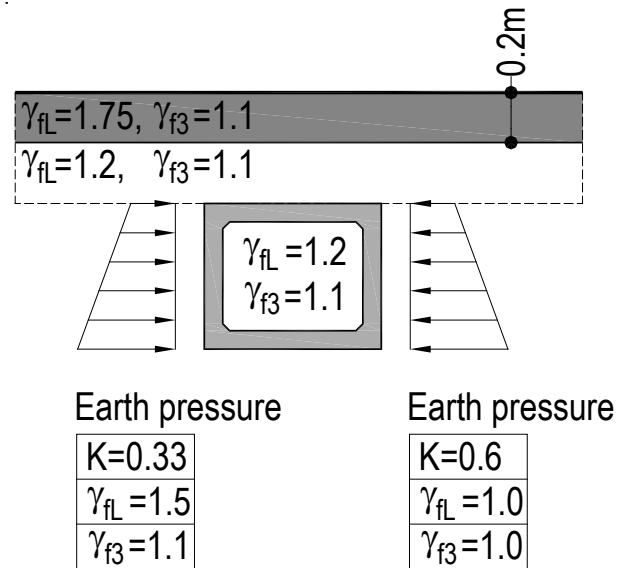


Figure 4: Partial load factors consistent with diagram A/4a [8].

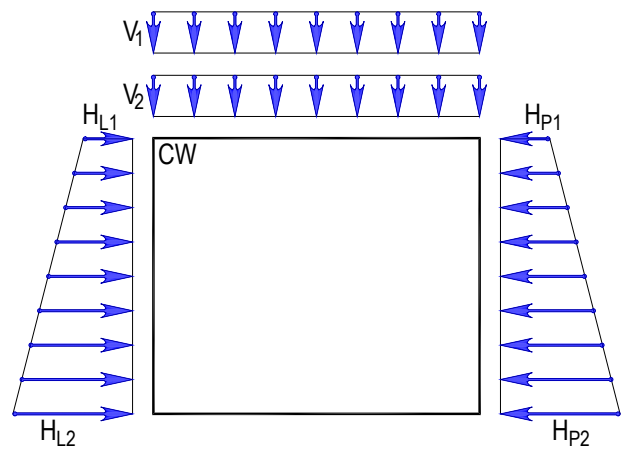


Figure 5: Load denotations and load action directions.

provides seven diagrams showing different load cases, which need to be considered in the design. The partial load factors for these loads are given in Figure 4. The calculated values of the loads and their denotations are shown in Table 3 and Figure 5. It is worth noting that loads such as load effects due to temperature, live load associated with traction, horizontal live loads, and other loads in the standards [8,10] as well as their combinations were not taken into account in the analysis. These loads additionally affected the values and distribution of internal forces in the bridge structure. Therefore, only for clarity of the analysis, the permanent loads were selected for the analysis.

Table 3. Permanent load.

Load		Values [kN/m]
Road pavement	V_1	$2.3 \cdot 0.2 \cdot 9.81 \cdot 1.75 \cdot 1.1 = 8.7$
Surcharge over bridge	V_2	$2.0 \cdot 1.1 \cdot 9.81 \cdot 1.2 \cdot 1.1 = 28.5$
Earth pressure behind left abutment wall	H_{L1}	$(2.3 \cdot 0.2 + 2.0 \cdot 1.1) \cdot 9.81 \cdot 0.33 \cdot 1.5 \cdot 1.1 = 14.2$
	H_{L2}	$(2.3 \cdot 0.2 + 2.0 \cdot (1.1 + 5.9)) \cdot 9.81 \cdot 0.33 \cdot 1.5 \cdot 1.1 = 77.2$
Earth pressure behind right abutment wall	H_{P1}	$(2.3 \cdot 0.2 + 2.0 \cdot 1.1) \cdot 9.81 \cdot 0.6 \cdot 1.0 \cdot 1.0 = 15.7$
	H_{P2}	$(2.3 \cdot 0.2 + 2.0 \cdot (1.1 + 5.9)) \cdot 9.81 \cdot 0.6 \cdot 1.0 \cdot 1.0 = 85.1$
Self-weight of concrete	CW	$2.4 \cdot 1 \cdot 0.45 \cdot 9.81 \cdot 1.2 \cdot 1.1 = 13.99$

Table 4. Concrete modulus of elasticity and Poisson’s ratios [11].

Member		
Bottom slab, concrete C32/40	E_{cm}	33.34 [GPa]
	ν	0.2
Abutment walls, upper floor slab, concrete C40/50	E_{cm}	35.22 [GPa]
	ν	0.2

Table 5. Model and parameters analyzed.

Model	k_h [kN/m ³]	k_v [kN/m ³]
M-1	10,000	10,000
M-2	37,000	10,000
M-3	120,000	10,000
M-4	10,000	80,000
M-5	37,068	80,000
M-6	120,000	80,000
M-7	10,000	120,000
M-8	37,000	120,000
M-9	120,000	120,000
M-10	0	∞

5 Soil parameters

In the calculations, the structure was assumed to be founded on Winkler’s unidirectional subgrade model. The elastic constraints connecting the bottom slab and abutment walls with the soil are only compression-loaded. This means that parts of the structure can detach from the surrounding soil. The superposition principle cannot be used in the calculations because of the nonlinear character of the bridge model supports. For this reason, all the loads involved were scaled up by applying a partial load factor and incorporated into a single load case. Ten numerical models were built. For clarity of the

analysis, it is assumed that the effective angle of shearing resistance f' is constant in all considered models. The variable parameters in the analyses are the modulus of subgrade reaction k_v applied under the bottom slab and the modulus k_h applied to the abutment walls. The first nine models are founded on a flexible subgrade. This was accomplished by applying to these models flexible constraints under the bottom slab and to the abutment walls. In addition, the values of modulus of subgrade reaction used for the bridge structure design are used in the model M-5. The geotechnical parameters used in this model were obtained from geotechnical investigations. The investigations were carried out for the native soil on which the bridge is founded and for the backfill used to bury the structure. The last model M-10 is founded on a rigid substratum such as a bedrock. This was accomplished by applying a pinned and rollers supports at the bottom slab. In addition, backfill stiffness behind the abutment walls is not included in this model. Owing to the ten models differing in only their support method, one can estimate the effect of the surrounding soil on the values and distribution of bending moment in the bridge structure elements. Models denotations and its parameters are shown in Table 5.

Abaqus FEA software was used for the structure analysis [16]. The calculations of the modulus of the horizontal reaction of the subgrade behind the bridge abutment walls were carried out according to Ménard’s empirical formula given in [17]. An example of calculations for the model M-5 is given below. The remaining values in Table 5 were adopted for the extreme values of medium dense and dense sand given in the publication [7].

$$k_h = \frac{3E_p}{\left(1,3r_0 \left(2,65 \frac{r}{r_0}\right)^\alpha + \alpha r\right)}$$

where:

Table 6. Stiffness of elastic constraints for M-5 model.

Symbol	Range of influence [m]	Modulus of subgrade reaction [kN/m ³]	Stiffness of elastic constraints [kN/m ²]
k_1	0.3375	$k_h = 80,000$	$0.3375 \cdot 80,000 = 27,000$
k_2	0.3625		$0.3625 \cdot 80,000 = 29,000$
k_3	0.5		$0.5 \cdot 80,000 = 40,000$
k_4	0.3375	$k_v = 37,068$	$0.3375 \cdot 37,068 = 12,510$
k_5	0.3625		$0.3625 \cdot 37,068 = 13,437$
k_6	0.5		$0.5 \cdot 37,068 = 18,536$

- k_h Modulus of horizontal subgrade reaction (backfill material)
- a, b Coefficients dependent on soil type and consistency, e.g. gravel $a = 1/4$, $b = 1/2$
- E_p Pressuremeter modulus of soil, $E_p \approx \beta q_c$
- q_c Cone soil penetration resistance determined by cone penetration test (CPT)
- r_0 Reference radius, $r_0 = 0.3\text{m}$
- D Bridge abutment wall height, $D = 5.9\text{m}$,
- r Radius, a half of abutment wall height $r = D / 2 = 5.9 / 2 = 2.95\text{m}$

Geotechnical investigation carried out using the CPT probe showed that the cone resistance for the backfill used on the construction site amounted to $q_c \approx 40,000\text{ kN/m}^3$. Hence, the calculated pressuremeter modulus of the soil was:

$$E_p \approx 40,000 \cdot 0.5 = 20,000\text{ kN/m}^3$$

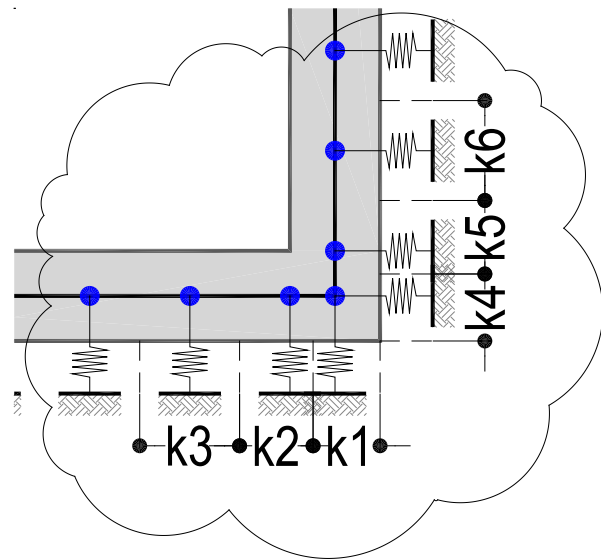
Substituting the above data into the Ménard formula for modulus k_h , the following was obtained:

$$k_h = \frac{3 \cdot 20000}{\left(1.3 \cdot 0.3 \left(2.65 \frac{2.95}{0.3}\right)^{0.25} + 0.25 \cdot 2.95\right)} = 37068\text{ kN/m}^3$$

The above is the modulus of the horizontal reaction of the subgrade behind the bridge wall. The modulus of the vertical reaction of the subgrade on which the bridge was to be built amounted to:

$$k_v \approx 80,000\text{ kN/m}^3$$

After these moduli had been determined, their values were proportionally distributed on the bridge model's abutment walls (k_h) and on bottom slab (k_v). The calculated values

**Figure 6:** Elastic constraints location.

of individual elastic constraints and their application in the nodes of the bridge model are presented on the example of the model M-5 and are shown in Figures 6, 7 and Table 6. The values of elastic constraints for the remaining models were calculated in the same way as for the model M-5. In the first nine models calculated, constraints (springs) are exclusively compression-loaded. The modulus of the horizontal subgrade reaction (k_h) was assumed to be constant along the height of the abutment walls.

Many factors, such as the soil classification its properties, initial soil state, the load type (short/long term), and its intensity and the shape and the size of the foundation, have influence on the value of the modulus of subgrade reaction. Short-term loading and unloading of the soil without occurrence of the consolidation and deconsolidation usually cause less settlement in it compared to when long-term static loading is acting on the

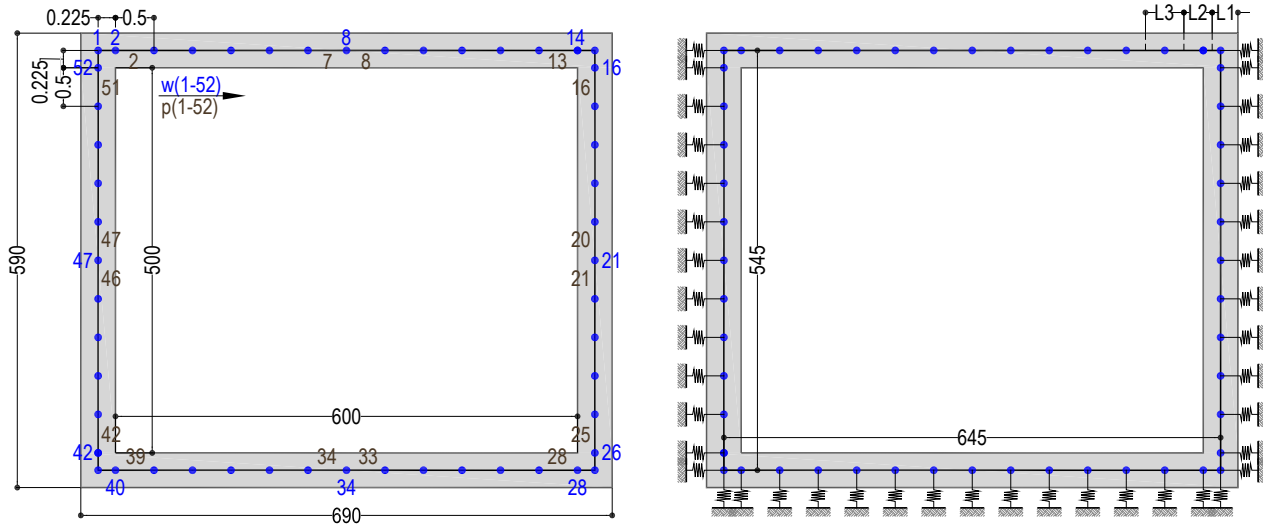


Figure 7: Beams and nodes location and elastic constraints distribution in cross-section.

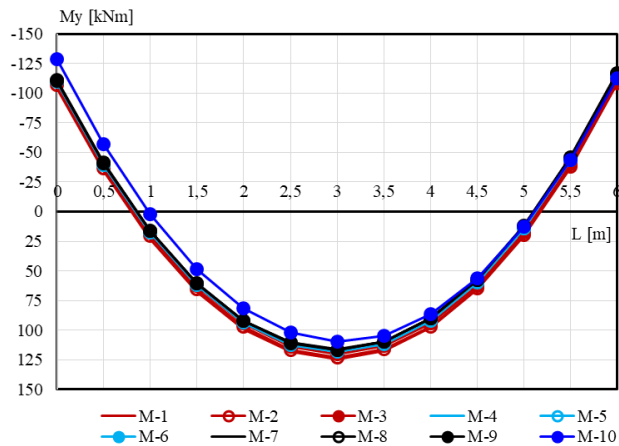


Figure 8: Distribution of bending moments in bridge's upper floor slab.

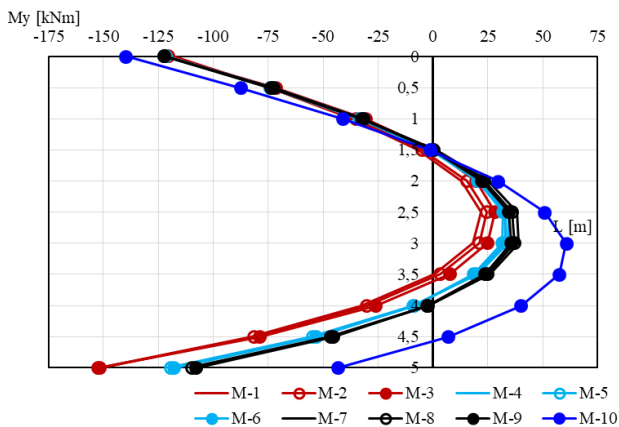


Figure 9: Distribution of bending moments in bridge's left abutment wall.

soil. For this reason, the value of the soil dynamic modulus E_d is usually higher than the initial elastic modulus E_0 of the same soil subjected only to static loads [6]. Wider and larger area loadings will involve consolidation of the deeper soil layers. The foundation's rigidity affects the stress distribution under the foundation. It should be emphasized that to properly determine the soil parameters for the structure design, close cooperation is necessary between the geotechnical and the structural engineer.

6 Bending moments

The bending moment values M_y were used in the parametric analysis. Graphs of the bending moments for the individual components of the bridge are shown in Figures 8–11.

The parametric analysis shows that the values of bending moments M_y at the midspan of the upper floor slab are higher in all models, taking into account subgrade and backfill stiffness than in the model M-10 supported on a rigid substratum. Whereas, in the region at the abutment walls, the reverse is the case. Subgrade and backfill stiffness have an impact on the values and distribution of bending moments in the upper slab of the analyzed bridge model. If subgrade and backfill stiffness are not taken into account in the bridge model, this can lead to excessive deflections and cracking of the upper floor slab at its midspan and to the over-reinforcement at the regions of the slab close to the abutment walls.

Bending moment values and their distribution in the abutment walls of the analyzed bridge model are mainly

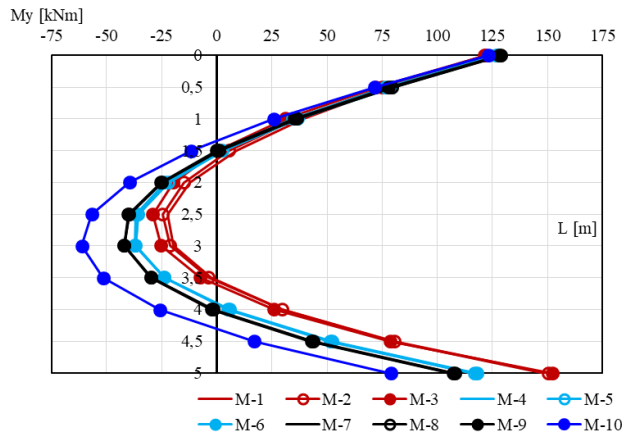


Figure 10: Distribution of bending moments in bridge's right abutment wall.

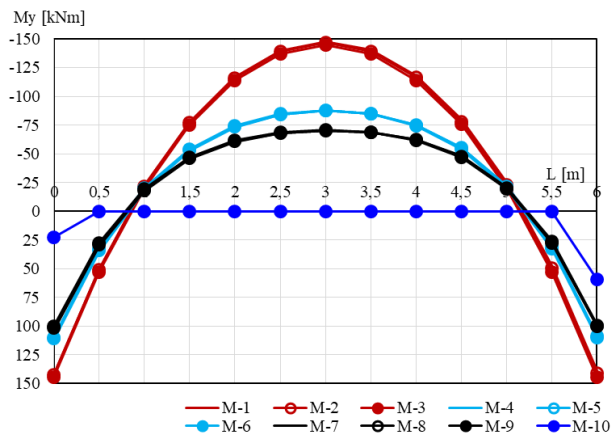


Figure 11: Distribution of bending moments in bridge's bottom slab.

Table 8. Bending moment values used for bridge design.

Member	Value [kNm]
Upper floor slab, midspan	362
Upper floor slab, at support	333
Bottom slab, midspan	196
Bottom slab, at support	287
Abutment wall at midspan	182

influenced by subgrade stiffness under the bridge. Backfill stiffness has small impact on bending moment values and their distribution in the abutment walls. Lower value of the modulus of subgrade reaction k_v cause an increase of bending moment values in the lower region of the abutment walls and a decrease of bending moment values

in their midspan region. Higher value of the modulus of subgrade reaction k_v causes the opposite. Moreover, in the midspan of the abutment walls, bending moment values M_y are lower in the models that take subgrade stiffness into account than in the model on a rigid substratum. The reverse is true for the lower region of the abutment walls close to the bottom slab, where bending moment values M_y are higher in the models taking into account subgrade stiffness. The highest bending moment value in the lower regions of abutment walls was obtained in the model M-3, and the lowest in the model M-10. In the upper region of the abutment walls, bending moment values are very similar in all models taking into account subgrade and backfill stiffness. If subgrade and backfill stiffness are not taken into account in the bridge model, this can lead to excessive cracking of the lower part of the abutment walls surfaces from the embankment side close to the bottom slab and to the over reinforcement of the walls at the midspan region.

Over the entire length of the bridge's bottom slab, bending moment values M_y are higher in all models that take subgrade stiffness into account than in the model supported on a rigid substratum. Higher values of subgrade stiffness k_v , cause lower bending moment values over the entire length of the bottom slab. Backfill stiffness has small effect on the bending moment values in the bottom slab. If subgrade stiffness k_v is not taken into account in the bridge model, this can lead to excessive cracking of the top surface at the midspan region and the bottom surface of the slab close to the abutment walls. Bending moment values in models M-1 to M-3 are very similar. The same is true for models M-4 to M-6 and models M-7 to M-9. In the bottom slab modeled on elastic subgrade, the highest bending moment value in the midspan, occurs in the model M-1 while the lowest is in the model M-9. In the model M-10 modelled on a rigid substratum, the bending moment values are zero at this location. At both ends of the bottom slab modeled on elastic subgrade, the highest bending moment values occurs in the model M-3 and the lowest is in the model M-9. In the model M-10 modeled on a rigid substratum, bending moment value in the bottom slab at the abutment walls region is 59 kNm, and it is equal to a half value obtained in the model M-9 in the same location. The bending moment values for which the bridge was designed are given in Table 7.

7 Conclusions

The bridge was put into service in the first half of 2010. After three years of bridge exploitation, no major cracks were found on the bridge structure than those assumed in the calculations as well as uneven settlement of the structure.

The parametric analysis shows that when the bridge is designed with subgrade stiffness taken into account, one gets different values and distribution of bending moment than for the model on a rigid supports. Due to foundation of the bridge on a flexible subgrade, it was proper to include it in this bridge design. If the elasticity of the subgrade had not been taken into account in the numerical model, this could have led to excessive deflections and surface cracking in such bridge elements as the bottom surface of the upper floor slab, both surfaces of the bottom slab, and the inner surfaces of the abutment walls from the embankment side. It should be added that excessive cracking in the structure elements may appear on invisible surfaces such as the inner surfaces of the abutment walls or bottom slab from the embankment side and on the upper surface of the bottom slab, on which, for instance, a road surface may be built. Therefore, cracking of these elements may not be visible during bridge exploitation or during periodical inspections. This can lead to an unexpected structure failure or ultimately to construction disaster.

It should be emphasized that prior to design calculations that take subgrade stiffness into account the proper soil parameters for both the subgrade and the backfill must be determined. On the basis of such data the designer can build a numerical model of the structure founded on the specific subgrade stiffness. Therefore, close cooperation is required between the geotechnical and the structural engineer when designing this type of bridge. If one designs a bridge founded on a different subgrade than the target one (e.g., on a rigid subgrade), this can result in the over-reinforcement of some of the structural members and in the under-reinforcement of other structural members. After the inspection of the bridge and the other bridges on this motorway, it was concluded that it had been proper to take into account subgrade and backfill stiffness in the bridge calculations. It should be noted that the integral bridge presented here very well interacts with the surrounding soil, under applied permanent and live loads. Bridges of this type can have structural members with a smaller cross-section in comparison with conventional design solutions in which the structure–soil interaction is not taken into account. Consequently, they are cheaper to build than conventionally built bridges

owing to the reduced quantity of the materials used. In the author's opinion, integral bridges can and should be built in Poland because they are less expensive and take less time to build. One should take into account the fact that the ambient temperatures in Poland are different than on the British Isles, and therefore, it is necessary to investigate integral bridge structures in our climate conditions. Such research would give bridge engineers a deep insight into the behavior of this type of bridges, whereby their span could be gradually increased. It is worth noting that increasingly more valuable publications on integral bridges and viaducts appear in Poland [15]. This indicates a growing interest in such structures on the part of bridge engineers in Poland.

References

- [1] HELOWICZ A., Integral single-span viaducts made of prefabricated prestressed beams. Scientific Conference - Bydgoszcz-Krynica Zdrój 2015; (in Polish).
- [2] HELOWICZ A., Integral bridges with prefabricated prestressed beams - designer experience. Scientific and Technical Conference Prestressed and Post-tension Concrete Structures, Kraków 16-17 April 2015; (in Polish).
- [3] HELOWICZ A., Matière arch bridges– designer experience. Scientific Conference - Bydgoszcz-Krynica Zdrój 2016; (in Polish).
- [4] HELOWICZ A., Multi-span integral viaducts made of box girders - designer experience. Scientific Conference - Bydgoszcz-Krynica Zdrój 2017; (in Polish).
- [5] HELOWICZ A., Designing of small integral bridges and culverts - designer experience. Scientific Conference - Bydgoszcz-Krynica Zdrój 2019; (in Polish).
- [6] WIŁUN Z., Outline of geotechnics. Transport and Communication Publishers, 2000. ISBN: 832061354X; (in Polish).
- [7] BOWLES J. E. Foundation analysis and design. Fifth Edition. ISBN 0079122477.
- [8] BD31/01: 2001. Volume 2, Section 2, Part 12. The design of buried concrete box and portal frame structures. Design Manual for Roads and Bridges. The Stationery Office, London.
- [9] BA42/96: 2003. Volume 1, Section 3, Part 12. The Design of Integral Bridges. Design Manual for Roads and Bridges. The Stationery Office, London.
- [10] BD37/01: 2001. Volume 1, Section 3, Part 14. Loads for Highway Bridges. Design Manual for Roads and Bridges. The Stationery Office, London. ISBN 0115523545.
- [11] BS5400-04: 1990. British Standard. Steel, concrete and composite bridges – Part 4: Code of practice for design of concrete bridges. ISBN 0580184420.
- [12] National Road Authority in Irlandii, www.nra.ie.
- [13] Fehily Timoney and Company, Ireland. www.fehilytimoney.ie.
- [14] Manual of Contract Documents For Road Works. Volume 1. Specification for Road Works. National Road Authority. March 2000.

- [15] Furtak K., Wrana B., Integral Bridges. Transport and Communication Publishers, 2005. ISBN: 832061550X; (in Polish).
- [16] Abaqus FEA software, Dassault Systems, <https://academy.3ds.com>
- [17] Bruijn E., Plastic design of breasting dolphins. Delft University of Technology. Project number H32102/36.
- [18] Microsoft Bing Maps, <http://www.bing.com>.